Screech Suppression in Supersonic Jets

T.D. Norum*
NASA Langley Research Center, Hampton, Virginia

Screech from underexpanded supersonic jets has been investigated experimentally. Multiple screech modes, or stages, are found to be present at most jet operating conditions. The fundamental screech tone of each mode attains a maximum amplitude at about 20 deg from the inlet axis, with higher harmonics exhibiting multiple lobes. The directivity of each harmonic is predicted quite well from a stationary array of acoustic monopoles, with phasing between consecutive monopoles determined by the shock cell spacing and eddy convection velocity. Large reduction of screech amplitude can be obtained from modifications to the jet exit geometry, although the extent of this suppression is mode dependent.

Introduction

THE upstream noise radiation from a shock-containing supersonic jet is dominated by a broadband shock-associated noise along with one or more high amplitude tones known as jet screech. These tones dominate the spectra of cold model jets, and although there is little detailed published information on supersonic exhaust flow from aircraft engines, screech has been found to cause structural damage in flight.[1] Screech from model scale supersonic jets was first studied in detail by Powell,[2,3] who proposed a mechanism similar to that of the edge tone. Disturbances shed at the nozzle exit interact with the shock to create sound that travels back to the nozzle to generate additional disturbances. In this feedback process the shock cells are set into oscillation at the screech frequency. The relationship between the time scale of the feedback process and the frequency of the fundamental screech tone was confirmed by Poldervaart et al.[4] who varied the position of a reflector placed near the nozzle exit to enhance the screech. Hammitt[5] found that the shock cell oscillations occurred close to the natural frequency of the jet column oscillation, and that the flow could be stabilized by shielding the jet exit from the generated sound. Lush and Burrin[6] measured screech amplitudes at different angles to the jet and found results similar to those predicted from Powell's model. An extensive study of the shock cell system in circular jets was performed by Davies and Oldfield.[7] They suggest that the different screech modes (characterized by discrete jumps in screech frequency with changing pressure ratio) can be attributed to alterations in the development of the shock cell spacing.

The interaction of jet screech with the broadband component of shock noise has not yet been established. However, the study of the mechanisms of the broadband noise in the presence of high-amplitude screech tones is difficult, since both acoustic and aerodynamic fluctuations are dominated by the screech. Successful reduction of the amplitude of screech has been attained through the introduction of small protrusions (tabs) into the jet at the nozzle lip.[8,9] These tabs, however, also have the effect of modifying the shock structure within the jet.[10] Their influence on the broadband radiated noise is particularly severe with convergent-divergent nozzles, since supersonic flow over the protrusions sets up a secondary shock structure within the jet.[11] A method of reducing screech by tabs that do not protrude into the jet flow has recently been reported by Kozlowski and Packman.[12]

Presented as Paper 82-0050 at the AIAA 20th Aerospace Sciences Meeting, Orlando, Fla., Jan. 11-14, 1982; submitted Jan. 21, 1982; revision received June 11, 1982.

* Research Engineer. Member AIAA.

The current study is aimed at developing a sufficient understanding of the screech process so that the extent of screech suppression by nonintrusive means can be determined. Far-field acoustic measurements and flow visualization are used to investigate mode transition in detail. Powell's acoustic model for screech is tested quantitatively through detailed directivity measurements. Finally, the extent of screech suppression obtained through alteration of jet exit conditions is determined from screech amplitude comparisons.

Experiment

The tests were performed in a small anechoic chamber of internal dimensions $3.9 \times 3.3 \times 2.5$ m. Calibration using point source tones at frequencies to 50 kHz has shown this chamber to be free of reflections down to 0.2 kHz. The choked jets used to investigate screech issued from tubes of 6.22 mm i.d. (D). These tubes were then attached to similar stock tubing about 1.5 m in length that protruded through the chamber wall. This arrangement insured a fully developed turbulent velocity profile prior to the tube exit and permitted measurements at all angles to the jet without reflective interference from extraneous surfaces. A single ¼-in. microphone was used to obtain the acoustic signals. It was mounted on a small, digitally controlled traversing mechanism that could rotate about the jet exit plane.

Unheated, pressurized air was supplied through an upstream pressure regulator and flowmeter. Since the experimental arrangement disallowed a plenum chamber, the jet stagnation pressure was calculated from the measured flow rate by assuming uniform choked flow in the tube. Results are presented in terms of the shock parameter β, which for air is related to the pressure ratio by

$$\beta^2 = M_j^2 - 1 = 5(p_t/p_a)^{2/7} - 6 \tag{1}$$

where M_j is the fully expanded jet Mach number, and p_t and p_a are the jet stagnation and the ambient pressures, respectively.

The tubes used in this study are shown in Fig. 1. Unless otherwise noted, the results reported were obtained using the baseline configuration (tube 1 in Fig. 1), which had a lip thickness of $0.27D$. The remaining configurations were used to determine the effect of exit geometry on screech. A metal reflecting baffle and baffles made of sound absorbing material that could be attached to the lip of tube 1 are also shown in Fig. 1.

Pressure ratios tested ranged from just above the sonic condition, 1.9 ($\beta = 0$), to about 4.3 ($\beta = 1.25$). The microphone was positioned at $92D$ from the jet exit and measurements were taken between 5 and 165 deg from the inlet axis. A 1000-

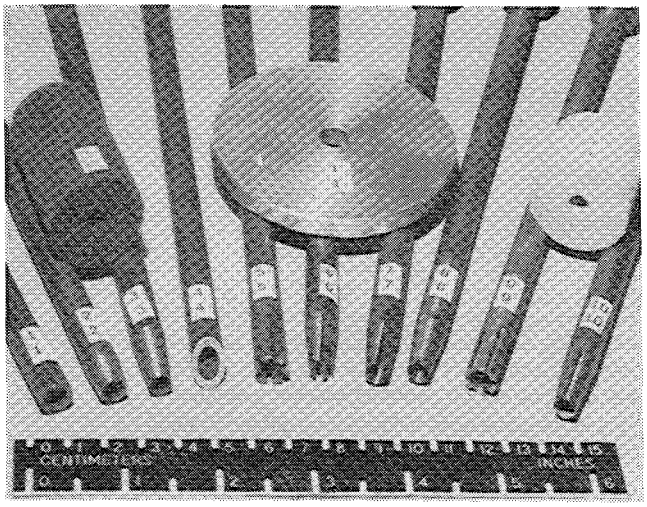

Fig. 1 Tubes and baffles for screech suppression study.

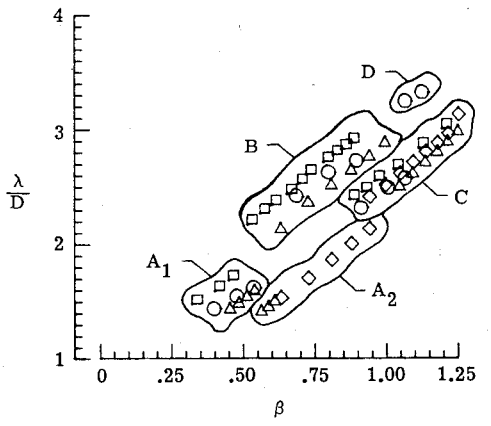

Fig. 2 Wavelength variations of the different screech stages from axisymmetric sonic nozzles. □ -Sherman[12]; ○ -Powell[3]; △ -Davies[6]; ◇ -Merle (as quoted in Ref. 6).

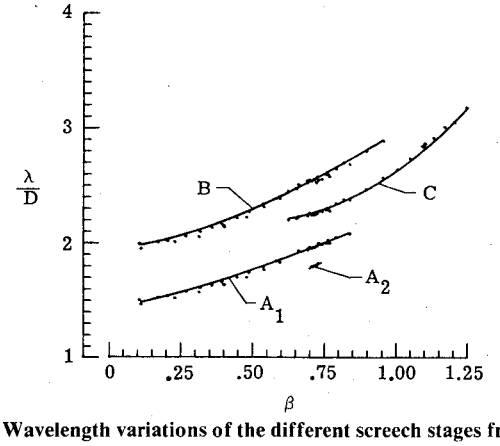

Fig. 3 Wavelength variations of the different screech stages from the baseline thick lipped tube.

line narrow-band spectrum to 120 kHz averaged over 15 s was processed for each run and stored on computer disk. Hence screech tone amplitudes presented represent the sound pressure level within a 120-Hz band containing the tone. About 1000 runs were obtained, each consisting of a given configuration β and measurement angle.

Shadowgraph visualization of the jet was obtained from a continuous point source derived from a mercury arc lamp. During this phase of testing the floor wedges of the chamber were removed for the shadowgraph equipment installation. Although the microphone remained in the chamber during visualization, its output was used only in the qualitative manner as discussed in the next section.

Different Stages of Screech

Previous experiments[3,7,13] on screech in axisymmetric supersonic jets give results that are qualitatively similar. As the pressure ratio is increased, the wavelength of screech increases until a critical point is reached at which a marked jump in wavelength occurs. This phenomenon repeats itself so that at least five separate modes have been identified. These modes have been labeled as stages A_1, A_2, B, C, and D. The results from these previous investigations are combined in Fig. 2. The wavelengths measured by the different investigators show reasonable scaling with jet exit diameter, although not all five modes were identified in each experiment.

Similar results were obtained for the current tests from narrow-band analysis of the acoustic signal measured at 20 deg from the inlet axis for configuration 1. As shown in Fig. 3, stages A_1, A_2, B, and C were identified with at least two of these existing at a given pressure ratio over most of the β range investigated. Additional screech tones not shown in Fig. 3, consisting of multiple harmonics of the mode's fundamental frequency were also present whenever the amplitude of the fundamental reached a level of about 100 dB.

Davies and Oldfield[6] found that shock cell development is qualitatively different within different pressure ratio ranges. Visualization during the current tests at the transition of dominant mode from stage B to stage C ($\beta = 0.7$) showed that the shock cell system switched back and forth between different states every few seconds. At the same instances the ear could detect a change in the quality of the noise generation. It was found that the jet could be stabilized in either state by placing a solid object such as one's hand at different locations near the jet exit.

To investigate this phenomenon further, the reflecting baffle was installed and moved from the plane of the jet exit to 6 tube diameters upstream of the exit. Spectra were obtained at $\beta = 0.7$ for each $0.1D$ increment of baffle location using a microphone at 20 deg from the inlet axis. It was found that for most baffle positions a single screech mode was dominant. However, the dominant mode changed between stages A_1, A_2, B, and C 13 different times as the baffle moved over the distance of 6 diameters. Stage B was dominant for over 50% of baffle positions, with the remainder being divided between stages A_1, A_2, and C. Shadowgraph visualization showed that for the baffle positions at which stage B was dominant, only about five shock cells could be observed, with the remainder of the shock cell system being obscured by large scale undulations of the jet. The baffle positions of stage C dominance showed about 8 cells visible, whereas from 9 to 11 cells were visible whenever either A stage dominated. At those few positions when two modes were of similar amplitudes, the shock cell system was seen to switch between the conditions corresponding to the two modes.

As the baffle position was changed over a small range in which a given mode was dominant, the measured screech frequency varied slightly, similar to that observed by Poldervaart et al.[4] As the baffle moved farther away from the exit the frequency decreased, indicative of a longer feedback cycle. After a 2-4% decrease in frequency, this screech tone decreased significantly in amplitude, and the jet locked onto a different screech mode. This process continuously repeated itself, with a given mode being dominant over a baffle distance ranging from 0.2 to $0.8D$.

There was no perceptible change in the spacing of at least the first four shock cells as the baffle was moved, although motion of the third and fourth cell ends was noticeable when stage B screech was dominant. The downstream shock spacings were hard to compare since they were obscured

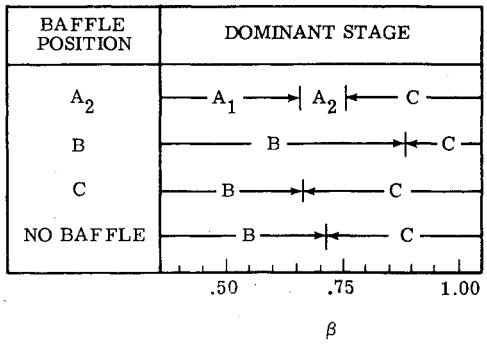

Fig. 4 Effect of baffle position on dominant stage of screech.

during the B mode. However, their apparent behavior was surmised by placing the baffle at a position where a sharp transition from stage A_2 to stage B occurred. As the baffle was "nudged," the downstream shocks of the A stage were seen to increase in length before becoming obscured by B stage undulations. The noticeable increase in downstream shock spacing at the onset of B stage screech may explain its longer wavelength. Since the feedback model of screech predicts wavelengths related to shock cell spacing, and only the downstream spacing is affected by mode, the primary sources of screech appear to be associated with the downstream shock cells.

Since these acoustic measurements were made in the presence of the shadowgraph equipment and the reflecting baffle, the measured screech amplitudes are no doubt influenced by shielding and reflections. Even so, the maximum screech amplitude at the 20 deg measurement angle appeared to be relatively independent of which mode dominated. The smallest peak amplitudes occurred at the baffle positions near mode transition, and, in fact, one position was found in which no screech tones could be observed in the spectrum. Of course, a generally increasing amplitude was obtained as the baffle was moved upstream, since less and less of the shock cell system was shielded from the microphone by the baffle.

To determine the influence of the reflecting baffle on mode stability at other pressure ratios, the baffle was placed at a position where stage B dominated at $\beta = 0.7$, and the pressure was varied from $\beta = 0.35$ to 1.0. This was repeated for baffle positions corresponding to C and A_2 mode dominance. The range over which each stage dominated for these different baffle positions is shown in Fig. 4. It can be seen that relative to the absence of the baffle, the B baffle position increases B stage dominance up to $\beta = 0.88$, and the C position extends C mode dominance down to $\beta = 0.66$. With the A_2 baffle position, B mode dominance cannot be found at any pressure ratio (in fact, low amplitude B tones could be distinguished in the spectra only over a very narrow range of pressure ratios near $\beta = 0.4$). Instead, the A_1 mode dominates to a much higher pressure, and the A_2 mode becomes the strongest stage over a small range near $\beta = 0.7$.

Since small differences in baffle position can have such a major effect on the measured spectra, differences in screech tone measurements by various investigators should be expected. Objects near the nozzle can change the amplification of the feedback process and at the same time influence the nature of the downstream shock development.

Directivity of Screech

Powell's[2] explanation of the screech process involves a feedback loop consisting of flow disturbances and sound waves. The disturbances are formed at the nozzle lip and travel downstream to interact with the shock structure. This interaction produces noise that travels upstream and creates additional disturbances upon passing the nozzle. This process led to an acoustic model of spacially stationary sources located at the ends of the shock cells, with phasing between them determined by the convection velocity of the disturbances. The far-field acoustic pressure resulting from this phased array of acoustic monopoles is

$$p = \sum_j \frac{S_j}{r_j} \exp\left[i \frac{2\pi c}{\lambda} \left(t - \frac{r_j}{c} - \frac{x_j}{U_c} \right) \right] \tag{2}$$

where λ is the wavelength of the screech tone, x_j is the distance from the nozzle exit to the source, r_j is the source to receiver distance, U_c is the disturbance convection velocity, c is the ambient sound speed, and S_j is related to the strength of the jth source. Utilizing the far-field approximation

$$r_j \simeq r_0 + x_j \cos\psi \tag{3}$$

where ψ and r_0 are the observer angle from the inlet axis and distance from the nozzle exit, and assuming an equal spacing L between sources, the pressure can be written as

$$p = \exp\left[\frac{i2\pi(ct - r_0)}{\lambda} \right] \sum_j \frac{S_j}{r_j} \exp\left[-i2\pi j \frac{L}{\lambda} \left(\frac{1}{M_c} + \cos\psi \right) \right] \tag{4}$$

Since the resulting far-field pressure is determined from the interference of terms within the summation, the directivity can be calculated if the disturbance convection Mach number, $M_c = U_c/c$, the source spacing to screech wavelength ratio, L/λ, and the number of sources and their relative strengths are known.

It can be seen from Eq. (4) that the signals from all sources are in phase and reinforcement occurs if

$$\frac{L}{\lambda} \left(\frac{1}{M_c} + \cos\psi \right) = n \tag{5}$$

where n is an integer. Since the feedback process depends on the amplitude of the sound impinging on the nozzle lip, it will be maximized if reinforcement occurs in the upstream direction ($\psi = 0$), and the screech wavelength is related to the cell spacing by

$$\lambda = \frac{L}{n} \left(1 + \frac{1}{M_c} \right) \tag{6}$$

Of course, the actual wavelength of the fundamental screech tone is a more complicated function of the various lengths involved in the feedback process. However, the wavelength must be close to that predicted by Eq. (6) for amplification to occur in the upstream direction.

The directivity of screech for a given β was obtained by traversing the microphone in an arc at a radius of $92D$ and measuring the spectra at least every 10 deg. At all pressure ratios for which directivities were obtained, the fundamental of the dominant mode peaked in the upstream direction at about 20 deg from the inlet axis. Higher harmonics could be found in the spectra when the level of the first harmonic (i.e., the fundamental) was greater than about 100 dB at this measuring location. The second harmonic generally dominates at 90 deg to the axis, and the higher harmonics contain the additional lobes typical of a phased array.

Measured directivities of the first four harmonics of the C screech mode at $\beta = 1.1$, and the first three harmonics of the B mode at $\beta = 0.65$ are given in Figs. 5 and 6. Also shown are directivities predicted from Eq. (4). In the computations the convection velocity was chosen to be 70% of the fully expanded velocity.[8,10] Also, since the spacing between the downstream shocks should be representative of the source spacing, and the shock spacing decreases with downstream distance, L was taken to be 90% of the length of the third

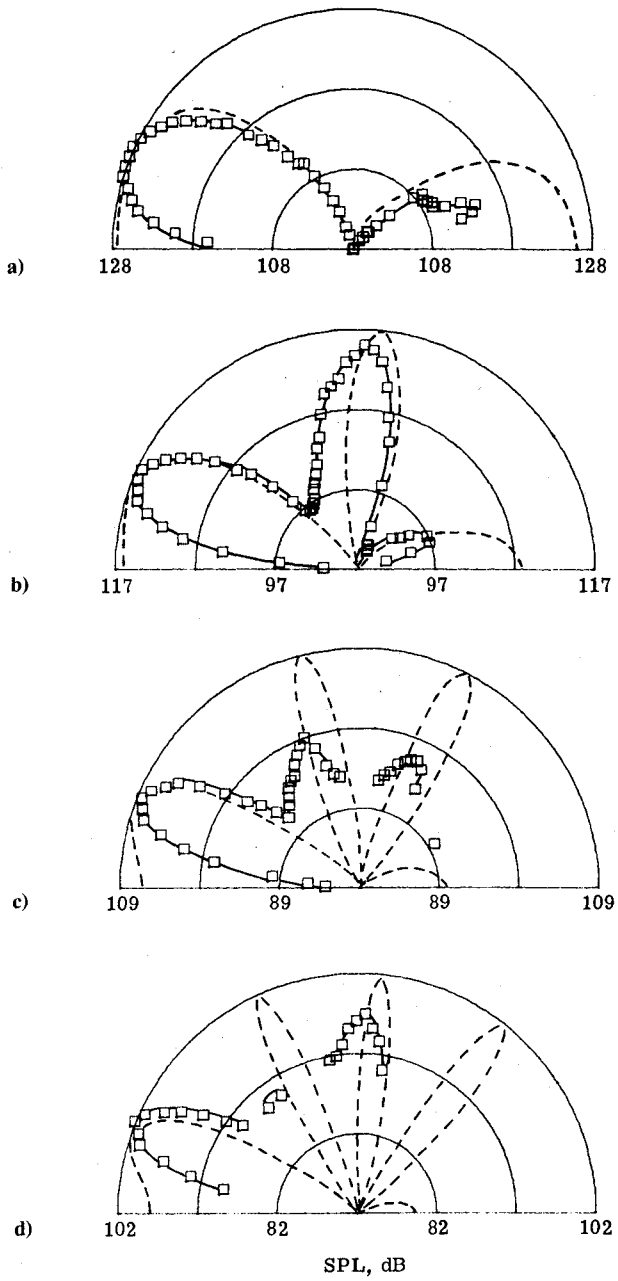

Fig. 5 Far-field directivity of C stage screech at $\beta = 1.1$; jet exhausts to the right; □——□ measured; --- predicted: $M_c = 0.87$, nine sources with parabolic strength variation; a) fundmental, $\lambda/L = 2.10$; b) second harmonic; c) third harmonic; d) fourth harmonic.

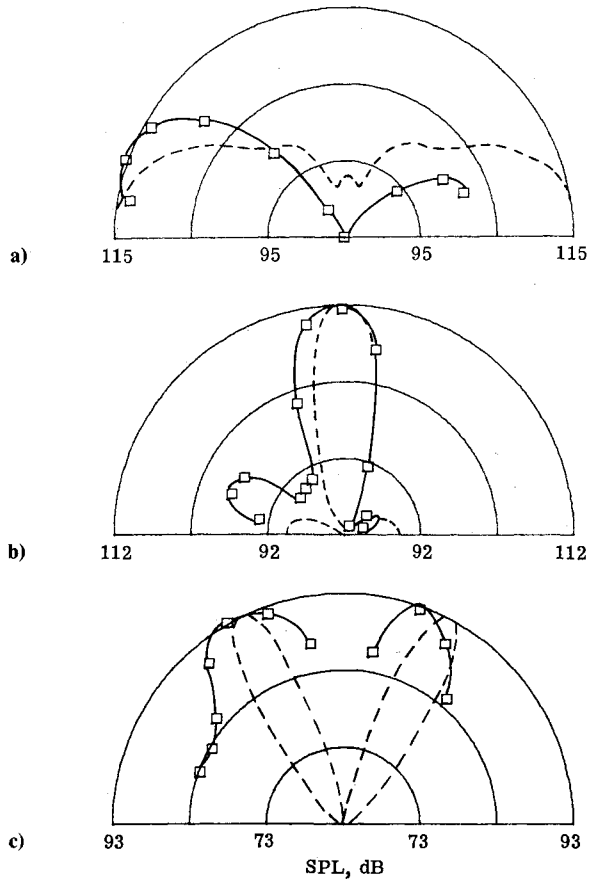

Fig. 6 Far-field directivity of B stage screech at $\beta = 0.65$; □——□ measured; ---predicted: $M_c = 0.74$, nine sources with parabolic strength variation; a) fundamental, $\lambda/L = 2.70$; b) second harmonic; c) third harmonic.

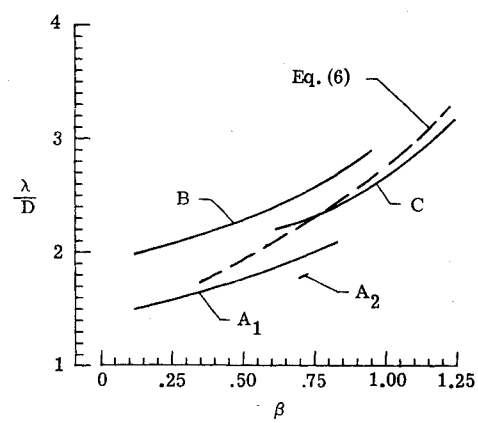

Fig. 7 Comparison of measured screech wavelengths with those predicted from Eq. (6).

shock cell as measured from the shadowgraph photographs. Nine monopoles were chosen with strengths decreasing parabolically from the central source, although these two parameters were found to have only minor effects on the relative amplitudes and widths of the lobes. (As few as three sources and no strength variation will yield the same general features in the predicted directivities.) However, M_c and L/λ have a strong effect on the shape of the predicted directivity pattern. Since the measured values of these parameters yield such good agreement between predicted and actual results for all harmonics of both cases, Powell's model is an excellent representation of the acoustic process.

The variation with β of the wavelength predicted from Eq. (6) (with $n = 1$) is shown in Fig. 7 along with the measured results. The computed wavelengths are very close to those measured for stage C screech. The fact that the predicted results fall within the range of measured wavelengths gives additional credence to the acoustic model.

Effects of Tube Exit Geometry

Since the feedback process of screech involves interaction of the generated noise with the nozzle exit, the effect of varying exit geometry on this process was investigated. Lip thickness was reduced to half that of the baseline configuration and to almost zero thickness (configurations 2 and 3 in Fig. 1). Symmetry of internal periphery was destroyed by beveling the tube end and by providing slots (configurations 4-8). External tabs were simulated through a grooved external surface (No. 9) and by attaching a small wire to the surface (No. 10). The metal reflecting baffle mentioned previously and the foam baffles shown in Fig. 1 were also used.

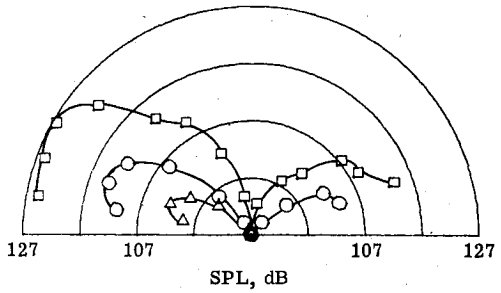

Fig. 8 Comparison of far-field directivities of fundamental screech tones at $\beta = 1.1$; □ -baseline thick lipped tube (No. 1); ○ -thin lipped tube (No. 3); △ -thin lipped tube with six long slots (No. 6).

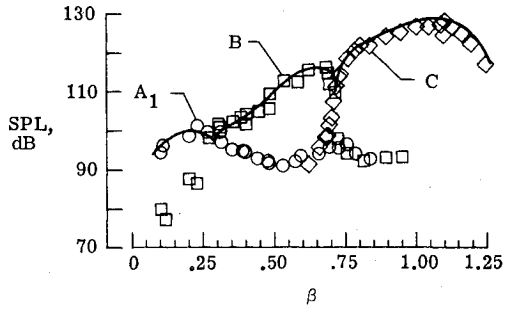

Fig. 9 Sound pressure level variations of the different screech stage fundamental tones from the baseline thick lipped tube; ○ -stage A_1; □ -stage B; ◇ -stage C.

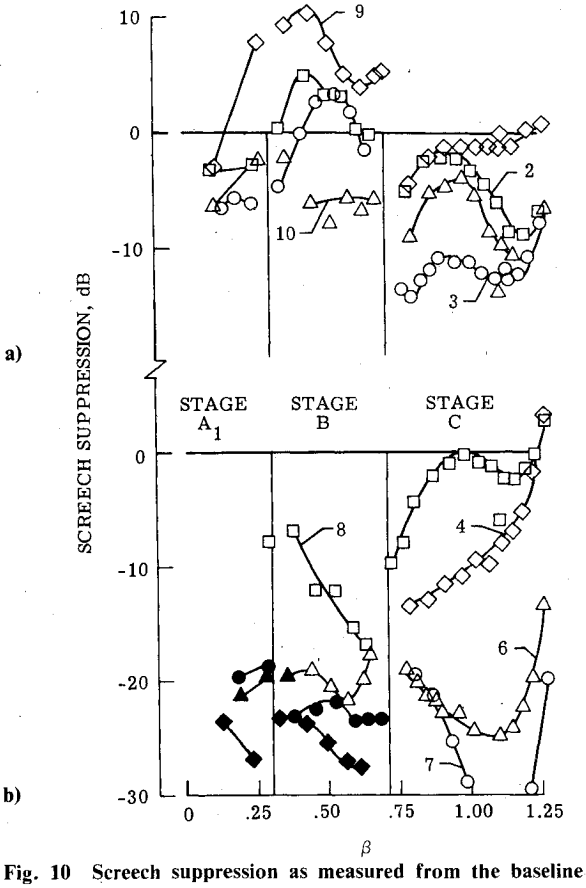

Fig. 10 Screech suppression as measured from the baseline thick lipped tube; a) □ -configuration 2; ○ -configuration 3; ◇ -configuration 9; △ -configuration 10; b) □ -configuration 8; ○ -configuration 7; △ -configuration 6; ◇ -configuration 4.

An example of how exit geometry can effect the strength of the screech process is shown in Fig. 8. The upstream directivity of the fundamental screech tone at $\beta = 1.1$ is shown for the baseline thick lipped tube (No. 1), the thin lipped tube (No. 3), and the thin lipped tube with long slots (No. 6). The shape of the directivity pattern is similar for the three configurations although the amplitude is reduced by about 10 dB when the lip thickness is eliminated, and another 10 dB when the periphery is disrupted.

Since the fundamental screech tone consistently appeared to peak at about 20 deg from the inlet axis, this angle was chosen to study the effects of exit geometry on screech. As the lip thickness was changed (Nos. 2 and 3), or when external tabs were simulated (Nos. 9 and 10), the screech wavelengths varied just like those of the baseline nozzle previously shown in Fig. 3. Consistent with this behavior, the shadowgraphs showed no differences in the appearance and spacing of the first few shock cells for any of these configurations.

This was not the case when continuity and/or symmetry of the internal wall was destroyed. The short slotted tube (No. 8) had small perturbations in the shock cell development and slightly smaller wavelengths for all three screech modes. The long slot of configuration 7 apparently relieved the internal pressure to such an extent that almost no shock cell development could be seen. A single low amplitude screech mode was measured only above $\beta = 0.6$. Its wavelength was between those of the C and B stages. Similar behavior was noted when additional slots were added around the periphery (No. 6). However, in this case the single low amplitude mode was observed down to $\beta = 0.4$. Low pressure screech was also not discernible for the beveled tube (No. 4), with a single mode existing at higher β with a wavelength somewhat smaller than the C stage. Although shocks could be seen in the jet, symmetry of the shock cell system about the jet centerline was completely destroyed.

The amplitudes of the A_1, B, and C modes as obtained from power spectra for the baseline configuration at 20 deg are shown in Fig. 9. The B mode dominates from $\beta = 0.3$ to 0.7, with stage A_1 dominating at lower pressure and stage C at higher pressure. Amplitudes are seen to be repeatable to within about ±2 dB. Screech suppression for any other configuration is defined as the maximum amplitude of its power spectrum minus the value obtained from the solid line of Fig. 9. Hence a negative value of suppression is a measure of the screech amplitude reduction relative to that of the baseline thick lipped tube.

The suppression obtained by varying lip thickness and introducing external tabs is shown in Fig. 10a. Reducing lip thickness (Nos. 2 and 3) is seen to decrease screech amplitude for the A and C modes, although very little overall effect is obtained during stage B. The thin lipped tube with external tab (No. 10) has a consistent 5-10 dB suppression, although it has higher amplitudes than the same tube without tab (No. 3) for all but the B mode. The grooved external surface configuration (No. 9) has very little screech suppression, and, in fact, appears to enhance screech at pressures below C stage dominance.

The screech suppression obtained from internal wall geometry changes is shown in Fig. 10b. (A solid symbol indicates that no screech tone was discernible; the suppression shown is measured to the peak of the broadband spectrum and hence is necessarily smaller than the unknown actual suppression.) The small slot (No. 8) increases the suppression over that obtained from the thin lipped configuration (No. 3) for the B mode, but appears to destroy the C stage suppression. The tubes with long slots (Nos. 6 and 7) show extensive screech suppression at all pressures, consistent with the shadowgraph evidence of very weak shock cell development and hence marked changes in the jet flow. Similar suppression is obtained with the beveled tube (No. 4), except for substantial increases in screech amplitude at high β.

The effect of the metal reflecting baffle on mode stability was described in a previous section. Its effect on the strength

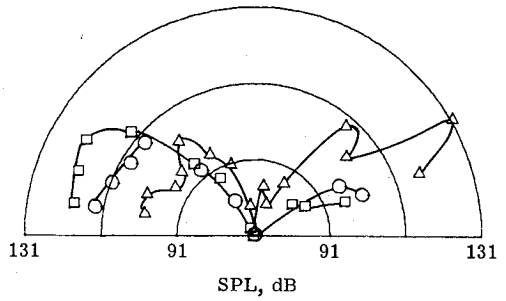

Fig. 11 Comparison of far-field directivities of fundamental screech tone at $\beta = 1.1$ for thick lipped tube with different baffles; □ -no baffle; ○ -foam baffle; △ -metal reflecting baffle.

of the screech process was investigated by positioning it flush with the tube exit, thus simulating an orifice flow (i.e., a nozzle lip thickness of many tube diameters). Additional tests were performed by replacing the reflecting baffle with a foam baffle (baffle 5 in Fig. 1) that slid over the tube, covered its lip, and extended $2D$ downstream of the exit. The directivity of the fundamental screech tone at $\beta = 1.1$ for the two cases is compared with that of the unbaffled configuration in Fig. 11. The reflecting baffle redirects the main lobe of the screech downstream. The amplitude at the position of maximum reinforcement is about 5 dB higher than the largest amplitude in the unbaffled case. This is consistent with the result obtained with increasing lip thickness. The foam baffle shows a slight reduction of screech in the upstream direction, although much smaller than the reduction obtained when the lip thickness was eliminated rather than covered (No. 3). Tests using a lower porosity baffle (baffle 4 in Fig. 1) and tests at other pressure ratios gave similar results on baffle effectiveness.

Conclusions

The nature of supersonic jet screech was investigated through experiments using a fully developed turbulent jet issuing from a small tube. The measured stages of screech agreed with those obtained from previous studies of convergent model scale nozzles. However, the amplitude of screech and the conditions for existence of a given mode were found to be highly configuration dependent. The visual and acoustic measurements obtained in this study yield the following specific observations.

1) A good correlation was found between the stage of screech and the stability of the jet as viewed from shadowgraph indications of the number of visible shock cells. Large scale changes in the jet flowfield appeared to occur at the instant of mode transition. Existence of multiple stages of screech for a given configuration and operating condition indicates that these changes can occur randomly with time. For a wide range of pressure ratios, the existence of a given screech mode was highly dependent on the position of a reflecting surface near the jet exit. Hence screech appears to be very sensitive to small changes in the parameters of the feedback loop that control the process.

2) The acoustic model for screech consisting of a phased array of monopoles located at the ends of adjacent shock cells was compared to experiment. The fundamental screech tone invariably peaked in amplitude in the upstream direction, with the existence of higher harmonics being dependent on the strength of the process. The predicted lobes in the directivity patterns showed excellent agreement with measurements for all harmonics, indicating that the model is a correct representation for the generation of screech tones.

3) Small modifications to the external surface of the tube at the jet exit had a large effect on the strength of the screech process. Although somewhat mode dependent, decreasing lip thickness yields lower screech amplitudes. Addition of an external tab did not reduce screech except for the most unstable mode, stage B. In general, screech amplitude appears to be dependent on the amount of solid surface area near the jet exit.

4) Modification of the internal surface of the tube had even greater effects. A small slot in the periphery decreased screech amplitude only for the B stage; however, larger slots yield extensive suppression for all screech modes. This suppression appears to depend on the degree of change to the axisymmetric shock cell development caused by the interruption of internal periphery.

References

[1] Hay, J.A. and Rose, E.G., "In-Flight Shock Cell Noise," *Journal of Sound and Vibration*, Vol. 11, April 1970, pp. 411-420.

[2] Powell, A., "On the Noise Emanating from a Two-Dimensional Jet Above the Critical Pressure," *Aeronautical Quarterly*, Vol. IV, Feb. 1953, pp. 103-122.

[3] Powell, A., "On the Mechanism of Chocked Jet Noise," *Proceedings of the Physical Society of London*, Sec. B, Vol. 66, 1953, pp. 1039-1056.

[4] Poldervaart, L.J., Vink, A.T., and Wijnan A.P.J., "The Photographic Evidence of the Feedback Loop of a Two-Dimensional Screeching Supersonic Jet of Air," *The 6th International Congress on Acoustics*, Tokyo, Japan, Aug. 1968, pp. F101-F104.

[5] Hammitt, A.G., "The Oscillation and Noise of an Overpressure Sonic Jet," *Journal of the Aerospace Sciences*, Vol. 28, Sept. 1961, pp. 673-680.

[6] Lush, P.A. and Burrin, R.H., "The Generation and Radiation of Supersonic Jet Noise," AFAPL-TR-72-63, Vol. V, 1972.

[7] Davies, M.G. and Oldfield, D.E.S., "Tones from a Choked Axisymmetric Jet," *Acoustica*, Vol. 12, No. 4, 1962, pp. 257-277.

[8] Harper-Bourne, M. and Fisher, M.J., "The Noise from Shock Waves in Supersonic Jets," *Proceedings of the AGARD Conference on Noise Mechanisms*, AGARD CP-131, 1973, pp. 11-1 to 11-13.

[9] Tanna, H.K., "An Experimental Study of Jet Noise, Part II: Shock Associated Noise," *Journal of Sound and Vibration*, Vol. 50, Feb. 1977, pp. 429-444.

[10] Norum, T.D. and Seiner, J.M., "Location and Propagation of Shock Associated Noise from Supersonic Jets," AIAA Paper 80-0983, June 1980; also *AIAA Journal*, Vol. 20, Jan. 1982, pp. 68-73.

[11] Seiner, J.M. and Norum, T.D., "Experiments of Shock Associated Noise on Supersonic Jets," AIAA Paper 79-1526, July 1979.

[12] Kozlowski, H. and Packman, A.B., "Flight Effects on the Aerodynamic and Acoustic Characteristics of Inverted Profile Coannular Nozzles," NASA CR-3081, Aug. 1978.

[13] Sherman, P.M., Glass, D.R., and Duleep, K.G., "Jet Flow Field During Screech," *Applied Scientific Research*, Vol. 32, Aug. 1976, pp. 283-303.